

Durham Research Online

Deposited in DRO:

02 August 2013

Version of attached file:

Accepted Version

Peer-review status of attached file:

Peer-reviewed

Citation for published item:

Perner, K. and Moros, M. and Jennings, A. and Lloyd, J.M. and Knudsen, K.L. (2013) 'Holocene palaeoceanographic evolution off West Greenland.', *The Holocene*, 23 (3). pp. 374-387.

Further information on publisher's website:

<http://dx.doi.org/10.1177/0959683612460785>

Publisher's copyright statement:

The final definitive version of this article has been published in the Journal 'The Holocene' 23/3, 2013 © The Author(s) 2012 by SAGE Publications Ltd at The Holocene page: <http://hol.sagepub.com/> on SAGE Journals Online: <http://online.sagepub.com/>

Additional information:

Use policy

The full-text may be used and/or reproduced, and given to third parties in any format or medium, without prior permission or charge, for personal research or study, educational, or not-for-profit purposes provided that:

- a full bibliographic reference is made to the original source
- a [link](#) is made to the metadata record in DRO
- the full-text is not changed in any way

The full-text must not be sold in any format or medium without the formal permission of the copyright holders.

Please consult the [full DRO policy](#) for further details.

1 **Holocene palaeoceanographic evolution off West**
2 **Greenland**

3 K. Perner^{1*}, M. Moros¹, A. Jennings², J.M. Lloyd³, K.L. Knudsen⁴

4 1 Leibniz Institute for Baltic Sea Research Warnemuende, Department of Marine Geology, Germany

5 2 Instaar and Department of Geological Sciences, University of Colorado, Boulder, USA

6 3 Durham University, Department of Geography, UK

7 4 Department of Geoscience, Aarhus University, DK-8000 Aarhus, DK

8

9 *corresponding author: kerstin.perner@io-warnemuende.de

10 Keywords: benthic foraminifera, WGC, IC, EGC, ocean forcing, Holocene

11

12

13

14

15

16

17

18

19

20

21

22

23

24

25

26

27 **(A) Abstract**

28 Benthic foraminiferal assemblages from a core southwest of Disko Bugt
29 provide a Holocene perspective (last ~7 ka BP) on ice-sheet/ocean interactions
30 between the West Greenland Current (WGC) and the West Greenland ice sheet.
31 Changes in the fauna reveal significant variations in the water mass properties
32 (temperature and salinity) of the WGC through time.

33 From 7.3 to 6.3 ka BP, a relatively warm/strong WGC influences ice sheet melt
34 in Disko Bugt and causes enhanced meltwater production, resulting in low surface
35 water productivity. The most favourable oceanographic conditions occur from 5.5 to
36 3.5 ka BP, associated with 'thermal optimum-like' conditions, encompassing
37 minimum ice sheet extent in the Disko Bugt area. These conditions are attributed to:
38 i) reduced meltwater influence as the ice sheet is land based and ii) enhanced
39 contribution of warm/saline water masses from the Irminger Current to the WGC. The
40 transition into the late Holocene (last ~3.5 ka BP) is characterized by a cooling of
41 oceanographic conditions, caused by increased advection of cold/low-salinity water
42 masses from the East Greenland Current. A longer-term late Holocene cooling trend
43 within the WGC is attributed to the onset of Neoglacial cooling within the North
44 Atlantic region. Superimposed on this cooling trend, multi-centennial scale variability
45 within the WGC matches reconstructions from a nearby coring site in Disko Bugt as
46 follows: i) cooling at ~2.5 ka BP, linked to the 2.7 ka BP 'cooling event'; ii) a warm
47 phase centred at 1.8 ka BP, associated with the Roman Warm Period; iii) slight
48 warming between 1.4 and 0.9 ka BP, linked to the Medieval Climate Anomaly; iv)
49 severe cooling of the WGC after 0.9 ka BP, culminating at 0.3 ka BP during the Little
50 Ice Age.

51 We show that multi-centennial scale paleoceanographic variability along the
52 West Greenland margin is driven by ocean forcing, i.e. variations in the relative

53 contribution of Atlantic (Irminger Current) and Polar (East Greenland Current) water
54 masses to the WGC during the last ~7 ka BP, influencing ice sheet dynamics.

55

56

57 **(A) Introduction**

58 Over the past two decades a negative mass balance and increased surface
59 melting of the Greenland Ice Sheet (GIS), accompanied by enhanced acceleration of
60 many of Greenland's marine terminating outlet glaciers (e.g. Jakobshavn Isbræ,
61 Helheim, Kangerdlugssuaq) has been identified (Zwally et al., 2002; Rignot and
62 Kanagaratnam, 2006; Moon and Joughin, 2008; Joughin et al., 2008; Howat et al.,
63 2007, 2008; 2011; Straneo et al., 2010). Recent studies have suggested that ocean
64 forcing may exert an important control on modern ice sheet dynamics by the
65 influence of warmer ocean conditions (e.g. Thomas, 2004; Joughin et al., 2004;
66 Bindschadler, 2006; Holland et al., 2008).

67 The Disko Bugt region in West Greenland is a key area to investigate the
68 influence of ocean forcing on GIS behaviour. This region has a relatively wide shelf
69 area and contains high-resolution sedimentary archives with the potential for records
70 to obtain the interaction between oceanographic variability and ice sheet behaviour.
71 The modern hydrographic conditions of the region are dominated by the West
72 Greenland Current (WGC, Figure 1). The water mass composition of the WGC is
73 linked to the large-scale North Atlantic climate system. Recent studies show that on a
74 multi-decadal timescale, temperature changes within the WGC have a profound
75 impact on subsurface melting of Disko Bugt outlet glaciers (e.g. Jakobshavn Isbræ),
76 at least during the last 60 years (Holland et al., 2008; Rignot et al., 2010; Lloyd et al.,
77 2011). Ice sheet limits in central West Greenland are uncertain during the Last
78 Glacial Maximum (LGM), but it has been suggested that ice streams may have

79 extended to the shelf edge along deep cross shelf troughs in the Disko Bugt region
80 (see Funder et al., 2011 and references there in). Limited evidence reported re-
81 appearance of the WGC in Disko Bugt from c. 9 to 10 ka BP (Funder and Weidick,
82 1991; Lloyd et al., 2005). Marine (Lloyd et al., 2005; Hogan et al., 2011) and
83 terrestrial (Weidick and Bennicke, 2007; Briner et al., 2010; Young et al., 2011)
84 studies suggest that Jakobshavn Isbræ had retreated into the Isfjord by c. 7.8 ka BP.
85 There are, however, no high resolution records available spanning the period of ice
86 retreat (after 8 ka BP) and minimum ice sheet extent (6 to 4 ka BP; e.g. Weidick and
87 Bennike, 2007; Briner et al., 2010) documenting the paleoceanographic evolution of
88 Disko Bugt (West Greenland).

89 To assess and understand the link between oceanic forcing and ice sheet
90 dynamics, a longer-term palaeoceanographic perspective is needed. In this study we
91 aim to investigate the oceanographic conditions off West Greenland during the
92 important period when the ice sheet retreated from western to eastern Disko Bugt,
93 and subsequently into the Isfjord. Specifically we aim to assess the potential link
94 between ice margin retreat and ocean temperatures during this period. We focus on
95 a new marine sediment core, from the shelf southwest of Disko Bugt, spanning the
96 last c. 7 ka BP. The coring site is located directly below the flow path of the WGC and
97 is expected to record: i) meltwater influence from the GIS (received along the West
98 Greenland margin and from Disko Bugt; ii) shifts in the relative contribution of the
99 relatively warm/saline Atlantic (Irminger Current) and colder/fresher Polar (East
100 Greenland Current) water masses to the WGC. Paleoenvironmental reconstructions
101 are inferred from benthic foraminiferal assemblage data. We use groupings of
102 Atlantic and Arctic water species as a proxy to identify qualitative changes in bottom
103 water mass properties of the WGC (e.g. Lloyd et al., 2011; Perner et al., 2011). Our

104 marine based reconstructions will provide a high-resolution longer-term Holocene
105 perspective on the paleoceanographic development of Disko Bugt.

106

107 **(A) Modern environmental setting of Disko Bugt**

108 Disko Bugt is a large marine embayment (40,000 km²) in central West
109 Greenland (Figure 1). Shallow water depths, varying between 200 and 400 m are
110 typically found, with maximum water depths up to 900 m in Egedesminde Dyb, a
111 deep water trough of glacial origin (Long and Robert, 2003; Roberts and Long, 2005).
112 Jakobshavn Isbræ, one of Greenland's largest outlet glaciers, flows into Disko Bugt
113 and currently drains about 7% of the GIS (Bindshadler, 1984). The present day
114 oceanographic setting of West Greenland is dominated by the WGC, which is formed
115 by a combination of: i) relatively warm and saline Atlantic-sourced water from the
116 Irminger Current (IC), a side branch of the North Atlantic Current (NAC); ii) Polar-
117 sourced cold, low-salinity water from the East Greenland Current (EGC; Buch, 1981);
118 and iii) local meltwater discharge along the SW Greenland coast (Figure 1). The
119 WGC enters Disko Bugt from the southwest and flows northwards exiting primarily
120 through the Vaigat into Baffin Bay. A branch of the WGC is deflected into Baffin Bay
121 west of Disko Island, while the main current continues to flow along West Greenland
122 northward into northern Baffin Bay (Andersen, 1981; Bâcle et al., 2002; Ribergaard et
123 al., 2006). Temperature and salinity data from Disko Bugt (Andersen, 1981; Buch,
124 1981; Buch et al., 2004; Lloyd et al., 2006; Harff et al., 2007) show that the WGC
125 (3.5–4°C, 34.2–34.4 PSU) forms the bottom waters within the bay. Andersen (1981)
126 found no indications of admixture of deep Baffin Bay waters below 300 m water
127 depth, penetrating into Disko Bugt. Surface waters, however, are influenced by
128 meltwater flux from land, icebergs and the previous season's pack ice, as well as
129 relatively low-salinity polar surface water advected from Baffin Bay. At present, the

130 Arctic sea-ice edge, formed annually in Baffin Bay between September and March, is
131 found just north of Disko Bugt in spring (Tang et al., 2004) and influences the surface
132 water productivity in the area (e.g. Hansen et al., 1999; Levinsen et al., 2000).

133

134 **(A) Material and Methods**

135 This study focuses on the composite record of a multi and gravity core
136 obtained from site MSM 343300 (68°28,311'N/ 54°00,119'W Figure 1) southwest of
137 Disko Bugt (cruise MSM05/03 of the *R/V 'Maria S. Merian'*; Harff et al., 2007). The
138 multi core (length: 28.5 cm) and gravity core (total length: 1132 cm, this study
139 focuses only on the depths 0-400 cm) were retrieved from 519 m water depth in
140 Egedesminde Dyb.

141 Age control is provided by accelerator mass spectrometry AMS¹⁴C dates on
142 mollusc shells and benthic foraminifera (Table 1, Figure 2). The chronology of the
143 composite record (last 7 ka BP) is based on 17 AMS ¹⁴C dates. The AMS
144 radiocarbon dates were calibrated using the Marine09 (Reimer et al., 2009)
145 calibration curve in CALIB 6.0.2 (Stuiver and Reimer, 1993). Following the results
146 from Lloyd et al. (2011), we applied a marine reservoir age correction ΔR of 140 ± 35
147 years, which represents the modern ΔR value for the Disko Bugt area.

148 Foraminiferal analysis was carried out on a standard volume of 5 ml fresh
149 sediment, soaked in deionized water overnight and gently sieved at 63 μm just before
150 counting. Multi core samples were counted at 1-2 cm intervals and gravity core
151 samples at 4 cm intervals. Calcareous and agglutinated foraminifera were counted on
152 a squared picking tray and identified to species level under a stereomicroscope from
153 the wet residue $>63 \mu\text{m}$ to reduce the loss of the more fragile arenaceous species
154 caused by drying out of sediment. The total number of specimens counted per
155 sample ranges from 300 to about 750. The Shannon-Wiener Index (S(H)), a measure

156 of faunal diversity, was calculated separately for the total (S(H)total; Figure 3), the
157 agglutinated (S(H)agglutinated; Figure 4), and the calcareous (S(H)calcareous;
158 Figure 5) assemblage.

159 Sediment samples (1 cm interval) were wet sieved at the 63 and 200 μm grain
160 size fraction to determine the sand content. The fraction 63-200 μm is used as an
161 approximate measure of the WGC's current strength and sediments deposited in the
162 fraction $>200 \mu\text{m}$ provide indications of ice-rafted debris (IRD) deposited at the coring
163 site. Additionally, counts of IRD ($>2 \text{ mm}$) on X-ray images were carried out. The total
164 organic carbon (TOC) of the bulk sediment (2 cm interval) is determined indirectly by
165 subtracting the total inorganic carbon from the total carbon content.

166

167 **(A) Results**

168 **(B) Age model and lithology**

169 Sediments are composed of mottled olive/greenish grey to moderate olive
170 brown organic rich clay with occasional shell fragments and drop stones. The depth-
171 age model was fitted to the calibrated ^{14}C dates using mixed effect modelling
172 (Heegaard et al., 2005). The age model of the multi core is based on linear
173 interpolation between the AMS ^{14}C date at 26.5 cm depth (Table 1) and the modern
174 age of 2007, the sampling year, for the core top (see Lloyd et al., 2011). Figure 2
175 presents the age model for the last 7.3 ka BP of the gravity core. According to our
176 age model, a gap of c. 500 years exists between the multi and gravity core. Loss of
177 the upper sediments is presumably due to the gravity coring technique. The
178 sedimentation rate in the gravity core averages 0.44 cm/yr between 7.3 and 3.5 ka
179 BP, increasing to 0.85 cm /yr between 3.5 and 1 ka BP.

180 The content of IRD ($>2 \text{ mm}$ fraction) is low within the core, supported by low
181 values of the $>200 \mu\text{m}$ % fraction throughout the last c. 7 ka BP (Figure 2a). The

182 sand content (63-200 μm % fraction) averages about 8% between 7.3 and 7 ka BP,
183 then increases to maximum values between 7 and 6.3 ka BP (averages 25%; Figure
184 2b). From about 6 ka BP, there is a gradual decrease in the sand content, reaching
185 an average of about 5% after 3.5 ka BP. The TOC content is initially low with an
186 average of $\sim 1\%$ between 7.3 and 5.5 ka BP, then increases gradually, reaching an
187 average of about 2.5% after 2.5 ka BP (Figure 2c). X-ray radiographs (A. Jennings
188 unpublished data) reveal two turbidites in the record, one at ~ 3 ka BP (199.5-201.5
189 cm core depth; peak in sand content; 0.5% drop in TOC content) and one at ~ 5 ka
190 BP (291-296.5 cm core depth). Data from these depths have been excluded from the
191 record and the following discussion.

192

193 **(B) The benthic foraminiferal assemblage and ecology**

194 Benthic foraminifera were counted from 120 samples from the combined
195 cores. A total of 52 benthic foraminiferal species were identified: 17 agglutinated and
196 35 calcareous species (see Appendix I for complete faunal list). Both calcareous and
197 agglutinated specimens were well preserved and showed minimal evidence of post
198 mortem (dissolution) changes throughout the core. This is supported by relatively low
199 counts of test linings per sample (Figure 3). Following previous studies on high-
200 resolution sites from the Disko Bugt area (e.g. Lloyd et al., 2011; Perner et al., 2011),
201 we present changes in the total benthic foraminiferal assemblage (agglutinated and
202 calcareous assemblage) along with summary curves of a chilled Atlantic water group
203 (AtIW) and an Arctic water group (AW). These groupings are based on environmental
204 preferences of the species (associated directly or indirectly with salinity and
205 temperature) and are used to identify changes in the relative temperature and salinity
206 of the WGC associated with changes in the respective water mass composition
207 (IC/EGC influence) during the Holocene.

208 In Table 2, we present a list of species included in the AtlW and AW group
209 along with references supporting species allocations. The AtlW group includes
210 species such as *Islandiella norcrossi* and *Cassidulina reniforme* (calcareous) and
211 *Adercotryma glomerata*, *Reophax pilulifer*, and *Ammoscalaria pseudospiralis*
212 (agglutinated). In the presented study, *I. norcrossi* is the most abundant species of
213 the AtlW group, indicating a relatively strong IC component of the WGC. The highest
214 abundance of this species is associated with a stable salinity during the most
215 ameliorated oceanic conditions of the Holocene. The AW group includes species
216 such as *Cuneata arctica*, *Spiroplectammina biformis*, and *Textularia torquata*
217 (agglutinated) and *Elphidium excavatum* f. *clavata* and *Islandiella helenae*
218 (calcareous). These species are indicative of relatively fresh and cold water mass
219 characteristics (strong EGC component and/or local meltwater influence from the
220 GIS) within the WGC. The total benthic foraminiferal assemblage also contains
221 various productivity indicator species such as *Nonionellina labradorica*,
222 *Globobulimina auriculata arctica*, *Buccella frigida*, *Melonis barleeanus*, *Epistominella*
223 *vitrea*, *Stainforthia loeblichii*, *Trifarina fluens* and *Pullenia* sp. The occurrence of these
224 species is often related to high productivity at the sea surface, which enhances food
225 supply to the sea floor and the availability of more or less degraded/altered organic
226 matter within the sediments (e.g. Mudie et al., 1984; Caralp, 1989; Polyak and
227 Solheim, 1994; Jennings et al., 2004).

228 The relative abundance (%) of the dominant agglutinated and calcareous
229 species based on the total assemblage over the last 7.3 ka BP is presented in Figure
230 3. Based on changes within the total assemblage, along with changes in AtlW and
231 AW groupings, an informal subdivision into three zones (A-C) has been made. The
232 relative abundance (%) of the agglutinated and calcareous fauna is also plotted
233 separately in Figures 4 and 5. Additionally, we provide absolute abundance of the

234 agglutinated and calcareous fauna (plotted as total specimens counted per ml wet
235 sediment) separately in the supplementary section (Figure S1-agglutinated species;
236 Figure S2-calcareous species).

237

238 **(C) The agglutinated assemblage**

239 *Deuterammia ochracea* is the most abundant species of the agglutinated
240 assemblage during the last 7.3 ka BP ranging from 40 to 60%. This is a cosmopolitan
241 species that is found widely in Arctic and sub-Arctic environments and provides
242 limited information on paleoenvironmental change within this study. In zone A, from
243 7.3 to 6.2 ka BP, AW species (e.g. *C. arctica*, *S. biformis*) are relatively common
244 averaging 10% of the fauna. This suggests relatively cold and fresh bottom water
245 mass conditions. At about 6.5 ka BP, there is a slight increase in AtIW taxa (*R.*
246 *pilulifer*, *S. difflugiformis* and *A. pseudospiralis*, *A. glomerata*), which is possibly linked
247 to occurrence of relatively warmer water masses at that time.

248 In zone B, *E. advena* increases to 15-20% between 6.2 to 5.6 ka BP, and
249 *Cribrostomoides* sp. averages 10% during this time interval. A minor rise noted in AW
250 species at c. 6.3 ka BP suggests a short-term cooling and freshening of bottom water
251 conditions. From c. 5.5 to 3.5 ka BP, we find lowest occurrence of the AW group over
252 the period studied, which indicates minimum influence from either local meltwater
253 sources in Disko Bugt or from the EGC component to the WGC during this time
254 interval.

255 In zone C, from c. 1.7 ka BP onwards, we note a gradual rise in overall
256 abundances and diversity of agglutinated specimens (S(H) Index exceeds 1.5). AtIW
257 species (*A. glomerata*, *A. pseudospiralis*, and *S. difflugiformis* *Reophax* sp.) increase
258 rapidly from c. 1.6 ka BP, reaching peak abundance of about 30% (Figure 4).
259 Subsequently, from c. 1.6 to 1.3 ka BP, a slight reduction in abundance of this group

260 occurs to about 20%. AW species show a gradual increase from c. 1.5 ka BP,
261 reaching peak values of approximately 30% from c. 0.9 ka BP onwards indicating
262 subsequent freshening and cooling.

263

264 **(C) The calcareous assemblage**

265 Between 7.3 and 6.3 ka BP (zone A), AtIW species dominate (40-80%), but
266 co-occurrence with AW species (10-40%) presumably reflects mixed (warm and
267 fresh) bottom water conditions. The overall abundance of productivity indicator
268 species (e.g. *N. labradorica*, *B. frigida*) is relatively low through this interval.

269 Relatively high abundance of *M. barleeanus*, compared to following intervals,
270 suggests that relatively old/degraded organic material is present at the site, with
271 limited replenishment from surface productivity at this time. At c. 7 ka BP, peak
272 abundance of the AtIW group (Figure 5; S2) reflects relatively warmer bottom water
273 conditions.

274 In zone B, peak abundance of *N. labradorica*, centred at 6 ka BP, indicates a
275 prolonged period of high surface water productivity, causing enhanced supply of
276 fresh phytodetritus to the sea floor. A pronounced rise in AW species (e.g. *Elphidium*
277 *excavatum* f. *clavata*, *I. helenae*) is also noted with peak abundance at c. 5.5 ka BP,
278 suggesting possible bottom water cooling. Subsequently, a pronounced decline in the
279 abundance of *E. excavatum* f. *clavata* is noted, coinciding with an increase in AtIW
280 species. From about c. 5.5 to 3.5 ka BP, the AtIW group dominates the assemblage,
281 documenting relatively warm and ameliorated bottom water conditions in the area
282 (Figure 5; S2).

283 In zone C, we observe a rise in AW species, in particular *E. excavatum* f.
284 *clavata*, but also a minor increase in *I. helenae*, reaching a peak at c. 2.7 ka BP
285 indicating cooling of bottom water conditions. The abundance of the AtIW group

286 declines through this interval, although a sudden peak in abundance is seen at c. 1.8
287 ka BP, comparable to abundances found between c. 5.5 and 3.5 ka BP. This
288 indication of a relatively warm WGC is accompanied by low abundance of AW
289 species (e.g. *E. excavatum* f. *clavata*) at c. 1.8 ka BP.

290 The most prominent feature in the uppermost part of the record is the abrupt
291 decrease of *E. excavatum* f. *clavata*, *I. norcrossi* and *C. reniforme* from about 0.9 ka
292 BP onwards, implying a change to harsher environmental conditions than previously.

293

294 **(A) Discussion**

295 **(B) Long-term Holocene changes in oceanographic variability of the WGC**

296 Our new benthic foraminiferal record, from the shelf southwest of Disko Bugt,
297 illustrates the permanent influence of the WGC, influencing the oceanographic
298 conditions within the area over the last c. 7 ka BP. From our data, the grouping of
299 *AtlWcalc* and *AWagg* indicator species, we can extract two main factors that
300 influence water mass properties of the WGC over time: i) meltwater influence from
301 the GIS, received along the West Greenland margin and from local sources in the
302 Disko Bugt region; ii) shifts in the relative contribution of warm/saline Atlantic (IC) and
303 of colder/fresher Polar (EGC) water masses to the WGC. The variations in local
304 influence from the GIS and regional ocean forcing will be discussed below.

305

306 **(C) Meltwater influence from the GIS (7.3 to c. 6.2 ka BP) in the Disko Bugt area**

307 Post-glacial reappearance of the WGC is reported from the West Greenland
308 area and the Canadian Arctic already after c. 9 ka BP (e.g. Hillaire-Marcel et al.,
309 2001; Lloyd et al., 2005; Knudsen et al., 2008a; Ren et al., 2009; Jennings et al., in
310 prep.). Evidence from marine and terrestrial records suggest that the GIS retreated
311 from the shelf west of Disko Bugt to the eastern part of the embayment by c. 10.2 ka

312 BP (e.g. Long and Roberts, 2002; Long and Roberts, 2003; Lloyd et al., 2005; Young
313 et al., 2011).

314 Strong melting from the GIS, translated to runoff into the ocean, is reported
315 between 8 and 6 ka BP (Alley and Anandakrishnan, 1995), and is thought to be in
316 response to atmospheric forcing, i.e. pronounced temperature rise over the GIS
317 (Dahl-Jensen et al., 1998; Vinther et al., 2009). In addition to this proposed
318 atmospheric forcing, our reconstructions (zone A) provide evidence of an ocean
319 forcing, with a relatively warm WGC entering Disko Bugt from c. 7.3 to 6.3 ka BP,
320 which presumably supports ice sheet melt in the area. This lower part of the record
321 is also characterized by strong variability in the flow strength of the WGC, displayed
322 by the sand content (Figure 6c). Initially, between 7.3 and 7 ka BP, decreasing sand
323 content suggests a weaker flow of the WGC (Figure 6c). The fauna is dominated by
324 AtlW species, but with variable amounts of AW species, which presumably reflects a
325 mixed (relatively warm and fresh) WGC (Figure 3). A relatively weaker flow of the
326 WGC might be related to meltwater influence from the GIS, received during the travel
327 of the current along the West Greenland margin. This interval coincides also with
328 reduced deposition of biogenic carbon (Figure 6e; MD99-2322) and low abundance
329 of AtlW species on the East Greenland shelf south of Denmark Strait, attributed to
330 continuing and enhanced melting from the GIS (Jennings et al., 2011). Following this
331 initial period, from c. 7 ka BP, significant increase in sand content reflects a
332 strengthening of the WGC flow, and a maximum is seen between 6.5 and 6.3 ka BP
333 (Figure 6c). During this period, post-glacial initiation of deep convection is reported
334 from the Labrador Sea (Hillaire-Marcel et al., 2001). The relatively low TOC content
335 and relatively high abundance of *M. barleeanus*, feeding on altered organic matter
336 (e.g. Caralp, 1989), indicates low in situ marine productivity at this time. We postulate
337 that relatively warmer bottom water flow into Disko Bugt supports/enhances ice sheet

338 retreat and caused enhanced meltwater production that circulated within the
339 embayment at this time. In turn, this meltwater discharge influences surface water
340 productivity, which is translated into reduced concentration of foraminiferal tests
341 (Figure 3) and lower abundance of productivity indicator species feeding on fresh
342 phytodetritus (e.g. *N. labradorica*, Figures 5, S2). This influence of surface water
343 productivity is prominently seen, when comparing the relative abundance and
344 concentration (no. of specimens per ml) of the AtIW group (see Figure 3, red and light
345 red graphs).

346 The increased flow of the WGC, accompanied by a rise in the concentration of
347 the AtIWcalc (Figure 6d) from c. 7 ka BP, correlates with enhanced deposition of
348 biogenic carbon and an abrupt rise in AtIW species in a core from the southern
349 Denmark Strait after c. 7 ka BP, which Jennings et al. (2011) relate to a warmer and
350 stronger IC (Figure 6e). Our results suggests that meltwater runoff from the GIS
351 started to decline after 7 ka BP and had reduced influence on the water mass
352 composition of the WGC along the West Greenland margin. This is supported by
353 terrestrial reconstructions, which report a largely land-based ice sheet by c. 7 ka BP,
354 which had retreated behind its present margin in eastern Disko Bugt (Weidick and
355 Bennike, 2007).

356

357 **(C) Thermal optimum oceanographic conditions (6.3 to ~3.5 ka BP) in the Disko** 358 **Bugt area**

359 A significant shift in oceanographic conditions is observed from 6.3 ka BP
360 onwards (zone B). This period starts with a prominent peak in productivity, shown by
361 the dominance of *N. labradorica*, between 6.3 and 5.8 ka BP (Figure 5). This most
362 likely relates to enhanced surface water productivity leading to increased supply of
363 fresh phytodetritus (food supply) to the sea floor. Such a strong productivity event

364 indicates a shift in the time period, when Arctic sea-ice breakup occurs in spring
365 months at Disko Bugt. We assume that prior to c. 6 ka BP the Arctic sea-ice edge
366 was positioned further south of Disko Bugt and breakup of the sea-ice edge occurred
367 during summer months at Disko Bugt, causing a greater annual bloom over the core
368 site. This is further supported by the occurrence of *I. helenae* and *S. loeblichii*
369 between 6.3 and 5.5 ka BP (Figure 5; Polyak and Solheim, 1994). From c. 5.5 ka BP
370 onwards, the distribution of *N. labradorica* remains at a continuously relatively lower
371 level, suggesting reduced sea-ice edge influence southwest of Disko Bugt.

372 Geomorphological studies in the eastern Disko Bugt area report a largely land-
373 based ice sheet and reduced meltwater runoff from the GIS after c. 6 ka BP (Weidick
374 et al., 1991; Weidick and Bennicke, 2007; Briner et al., 2010). As the ice sheet in the
375 Disko Bugt area was now largely land-based, entrainment of the relatively warm
376 WGC into the embayment could have no direct impact on the ice sheet and force
377 enhanced melting. Consequently, local meltwater discharge from the GIS in the
378 Disko Bugt area will have a more limited influence on the oceanographic record at
379 our core site southwest of Disko Bugt. From this time onwards, the WGC presumably
380 displayed the dominant water mass in Disko Bugt, and it is likely to have influenced
381 surface water properties as well. Henceforth, shifts in abundance of the AtIWcalc and
382 AWagg groups would now indicate changes in the qualitative water mass
383 contributions from the WGCs source currents (EGC and IC, respectively). The overall
384 dominance of the AtIWcalc fauna, between c. 5.5 to 3.5 ka BP (Figure 6d), highlights
385 strong contribution from the IC, and hence a relatively warm and saline WGC in
386 Disko Bugt. A strong and relatively warm IC is also reported from the East Greenland
387 shelf (Figure 6e; Jennings et al., 2002; Jennings et al., 2011) and to the south of
388 Iceland during this time interval (e.g. Knudsen et al., 2008b).

389 Already after 6 ka BP, we observe decreasing current strength of the WGC at
390 the coring site by decreasing sand content to about 15% at 4.0 ka BP (Figure 6c).
391 The reduced flow speed of the WGC registered at the core site does not affect the
392 relative warmth of the WGC, as shown by the dominance and high concentration of
393 the AtlWcalc group at that time (Figure 6d). We assume that the main core of the
394 WGC moved away from the sea floor at the core site. This is accompanied by a slight
395 increase in sedimentation rate, coincident with a increasing TOC (%) content, which
396 is most likely related to enhanced in situ marine productivity at the sea surface
397 (Figures 6a, b).

398 Between c. 5.5 and 3.5 ka BP, we find low abundance of total AW species
399 (e.g. *E. excavatum* f. *clavata*; *C. arctica*, and *S. biformis*; Figures 4, 5, 6f), reflecting
400 minimum influence of cool freshwater either from the GIS meltwater and/or the EGC
401 during this period. Accordingly, regional oceanographic conditions had stabilized
402 between c. 5.5 and 3.5 ka BP and the warmest, most ameliorated oceanographic
403 bottom water conditions, reflecting ‘thermal optimum-like’ conditions prevailed. As
404 noted above, a relatively warm WGC was already present in the area from c. 7.3 ka
405 BP onwards, but until c. 5.5 ka BP, the regional oceanographic signal was
406 overprinted by the influence of ice sheet meltwater on the WGC at the site.

407 The faunal data, presented here, tend to support an interpretation of extended
408 ‘thermal optimum-like’ conditions from c. 7 to 3.5 ka BP. The assumption of a longer
409 optimum would be in accordance with previous reconstructions of thermal optimum
410 conditions from terrestrial and marine studies in the Disko Bugt area (Funder and
411 Weidick, 1991; Fredskild, 2000; Lloyd et al., 2007; Young et al., 2011). Relatively late
412 thermal optimum conditions in the bottom waters southwest of Disko Bugt also
413 supports the spatially variable nature of Holocene Thermal Maximum (HTM)
414 conditions, caused by local ice sheet melt influence (see discussion by Kaufman et

415 al., 2004; Kaplan and Wolfe, 2006). Nonetheless, increased occurrence of drift ice on
416 the North Iceland Shelf from 5.5 ka BP onwards (Figure 6g), attributed to an
417 expansion of the EGC, indicates a climatic shift, involving widespread circulation
418 changes in the high latitude North Atlantic (Figure 6g; Moros et al., 2006a). This
419 might consequently also affect the flow strength of the WGC southwest of Disko
420 Bugt.

421

422 **(C) Onset of Neoglacial cooling (3.5 ka BP to present)**

423 From about 3.5 ka BP onwards (zone C) the benthic foraminiferal assemblage
424 documents cooling/deterioration of the oceanographic/environmental conditions at
425 the core site. We observe cooling/freshening (increase in total abundance of
426 agglutinated specimens and AWagg fauna; Figure 6f) and weakening (decrease in
427 sand content; Figure 6c) of the WGC. This cooling trend is consistent with results
428 from a previous study of nearby coring site 343310 (Figure 1; Perner et al., 2011) and
429 is attributed to an enhanced influence of the EGC. This increased contribution of
430 relatively cold and fresh water masses to the WGC correlates with the onset of
431 Neoglacial cooling in West Greenland.

432 After 3.5 ka BP, the sedimentation rate increases from an average rate of 0.44
433 cm/yr to about 0.85 cm/yr, accompanied by a 1% rise in TOC content (Figure 6a, b).
434 This is linked to enhanced in situ productivity at the site, which may also be a
435 consequence of the notably weaker WGC, compared to the preceding intervals
436 (Figure 6c). The observed deterioration of environmental conditions, initiated around
437 3.5 ka BP, corresponds well with the reported termination of relatively warm
438 conditions on the NW Iceland Shelf (Jiang et al., 2002), in the Denmark Strait
439 (decrease in biogenic carbon content, Figure 6e; Jennings et al., 2011) and in
440 western/south Greenland (e.g. Fredskild, 1984, 2000; Bennike, 2000; Kaplan et al.,

441 2002; Kuijpers et al., 2003; Lassen et al., 2004; Moros et al., 2006b; Møller et al.,
442 2006; Seidenkrantz et al., 2007, 2008; Lloyd et al., 2007). In addition to this oceanic
443 cooling, terrestrial reconstructions suggest an advance of the GIS after 4 ka BP
444 within the Disko Bugt area (Weidick and Bennike, 2007; Briner et al., 2010, Young et
445 al., 2011), as well as cooling over the GIS (Dahl-Jensen et al., 1998), coinciding with
446 decreasing summer solar insolation (Berger and Loutre, 1991).

447 Superimposed on this late Holocene cooling trend we find multi-centennial
448 scale variability in the WGC, correlating with the variability reported by Perner et al.
449 (2011). A cooling around 2.5 ka BP (increased abundance of AW species *I. helenae*;
450 Figure 5, S2), is associated with the 2.7 ka BP ‘cooling event’, which has been
451 recorded in various marine and terrestrial records in the North Atlantic region (e.g.
452 Oppo et al., 2003; Risebrobakken et al., 2003; Hall et al., 2004; Moros et al., 2004). A
453 pronounced relatively warm phase is seen at 1.8 ka BP (marked increase in the
454 AtlWcalc fauna; Figure 6d), can be linked to the Roman Warm Period ‘RWP’. This
455 period records oceanographic conditions comparable to, or perhaps slightly warmer
456 than the ‘thermal optimum-like’ conditions seen between c. 5.5 and 3.5 ka BP of
457 West Greenland. Significant warming during the ‘RWP’ also correlates with findings
458 from the Reykjanes Ridge in the central North Atlantic (Moros et al., in press).

459 The gradual cooling of bottom water conditions, which becomes more
460 pronounced from ~1.8 ka BP onwards (gradual rise in AWagg species; Figure 6f),
461 indicates enhanced freshwater forcing from the EGC (cf. Perner et al., 2011) and
462 reduction in IC contribution to the WGC. Nonetheless, a minor warming of bottom
463 water conditions is seen between 1.4 and 0.9 ka BP (Figure 6d), which corresponds
464 to the ‘MCA’, suggesting a continuous significant IC contribution to the WGC during
465 this time period. The foraminiferal fauna shows that the ‘MCA’ warming is less
466 pronounced than that of the ‘RWP’, and it is also evident that the ‘RWP’ records the

467 warmest phase during the late Holocene (see Figure 6d; Perner et al., 2011).
468 Relative cooling of oceanographic conditions from the 'RWP' to the 'MCA', between
469 1.8 and 0.7 ka BP, agrees well with previous findings from the Disko Bugt area
470 (Perner et al., 2011) and with other marine records from the northern North Atlantic
471 (e.g. Andrews and Giraudeau, 2003; Moros et al., 2004, 2006a, in press; Richter et
472 al., 2009).

473 No sediments are recovered in the present record between 0.7 and 0.3 ka BP
474 (gap in composite record of core 343300). However, severe cooling is seen after 0.9
475 ka BP culminating in the 'Little Ice Age' at 0.3 ka BP related to a continuous increase
476 in the EGC component of the WGC (rise in overall abundance/diversity of
477 agglutinated species and the AWagg fauna, Figure 6f, and supplemented with data
478 from core 343310 (Perner et al., 2011); Figure 6d – light red line, 6f – light blue line).
479 Enhanced EGC contribution to the WGC during the 'LIA' is supported by studies from
480 the East Greenland Shelf, North Icelandic Shelf, Denmark Strait and Southeast and
481 West Greenland, reporting expansion and intensification of the EGC by enhanced
482 contribution of relatively fresher/colder Polar water masses and increased drift ice
483 (e.g. Figure 6g) within the EGC (Andrews et al., 1997; Kuijpers et al., 2003; Eiríksson
484 et al., 2004; Moros et al., 2006a; Jennings et al., 2011; Sha et al., 2011). This
485 oceanic cooling encompasses the reported re-advance of Jakobshavn Isbræ, to its
486 LIA maximum position, 20 km west of its current position (Weidick et al., 1990).

487 Reconstructions by Kaufman et al. (2009) from terrestrial archives document a
488 strong increase in arctic summer air temperature during the last c. 100 years.
489 Contrary to this our data show that oceanographic conditions (WGC) are relatively
490 cool and remained cooler during the last 100 years than during the 'MCA'. Similar
491 results were obtained by Sha et al. (2011) from a site further south on the West
492 Greenland Shelf. These environmental conditions are presumably determined by a

493 relatively strong contribution from the cold EGC during the last 100 years, and are in
494 agreement with the freshening of Baffin Bay between 1916-2003, reported by Zweng
495 and Münchow (2006).

496

497 **(A) Summary and Conclusions**

498 A new Holocene benthic foraminiferal record from southwest Disko Bugt
499 provides detailed information of multi-centennial scale bottom water (WGC) variability
500 off West Greenland and interaction of the WGC with the West Greenland ice sheet.
501 Our reconstructions provide a long-term Holocene perspective on the influence of
502 ocean forcing on the Greenland Ice Sheet in the Disko Bugt area.

503 Between c. 7 and 6.3 ka, we observe, a relatively warm and strong WGC,
504 which is likely to support ice sheet melt in Disko Bugt, leading to increased meltwater
505 production, and consequently results in low surface water productivity. A subsequent
506 strong productivity event at c. 6 ka BP suggests that the Baffin Bay Arctic sea-ice
507 edge migrated from its location to the south of Disko Bugt northwards across the site,
508 presumably linked to the influence of the relatively warm and strong WGC. A
509 prolonged relatively warm/stable phase of the WGC is indicated by persisting
510 dominance of the *AtlWcalc* fauna from c. 5.5 to 3.5 ka BP, reflecting 'thermal
511 optimum-like' conditions off West Greenland.

512 Most likely a relatively warm and strong WGC was continuously present on the
513 shelf of Disko Bugt during the entire period between c. 7 and 3.5 ka BP, albeit its
514 signal is diluted/deflected (overprinted) in our data by the melting ice sheet, which in
515 turn resulted in relatively cooler and variable environmental conditions.

516 From about 3.5 ka BP, benthic foraminifera identify a long-term late Holocene
517 cooling of the bottom waters, associated with the onset of Neoglacial cooling. This
518 indication of a long-term cooling agrees well with studies from West/East Greenland

519 fjord and shelf areas, which report gradual cooling of the WGC, along glacial re-
520 advances. It is likely that cooling of oceanographic conditions favoured the observed
521 re-advance of the ice sheet in the Disko Bugt area after c. 3.5 ka BP. Superimposed
522 on this cooling trend, we reconstruct marked multi-centennial scale variability within
523 the WGC: i) a cooling at c. 2.5 ka BP, related to the 2.7 ka BP 'cooling event'; ii) a
524 relatively warm phase at c. 1.8 ka BP, corresponding to the 'Roman Warm Period'; iii)
525 only a slight warming in bottom waters at the transition into the 'Medieval Climate
526 Anomaly' and; iv) strong cooling from c. 1.8 ka BP culminating in the 'Little Ice Age'
527 cold period.

528 Cooling of bottom waters, confirmed by a gradual rise in AWagg species, is
529 linked to an enhanced influence of fresher/cooler water mass contribution from the
530 EGC to the WGC. Agglutinated species dominate the benthic foraminiferal
531 assemblage also during the last 100 years, corroborating a persistent strong
532 influence of the EGC on the WGC, consistent with previous studies from Disko Bugt
533 and the West Greenland shelf.

534

535 **Acknowledgements**

536 The authors thank the Deutsche Forschungsgemeinschaft (DFG) for funding
537 the project 'Disko Climate' (MO1422/2-1). We also thank the Captain and Crew of the
538 R/V 'Maria S. Merian' for their fantastic work during cruise MSM05/03. We thank
539 Marit-Solveig Seidenkrantz for fruitful discussion of the benthic foraminiferal
540 assemblage and their interpretation, Tomasz Goslar from Poznań Radiocarbon
541 Laboratory and also Richard Telford from the University of Bergen, for performing the
542 age-depth modelling of the gravity core.

543

544

545 **(A) References**

- 546 Alley RB, Anandakrishnan S (1995) Variations in melt-layer frequency in the GISP2
547 ice core: implications for the Holocene summer temperatures in central
548 Greenland. *Glaciology* 21: 64-70.
- 549 Andersen OGN (1981) The annual cycle of temperature, salinity, currents and
550 water masses in Disko Bugt and adjacent waters, West Greenland.
551 *Meddelelserom Grønland, Bioscience* 5: 1-36.
- 552 Andrews JT, Smith LM, Preston R, Cooper T, Jennings AE (1997) Spatial and
553 temporal patterns of iceberg rafting (IRD) along the east Greenland margin,
554 ca.68 N, over the last 14 cal. ka. *Journal of Quaternary Science* 12: 1-13.
- 555 Andrews JT, Giraudeau J (2003) Multi-proxy records showing significant Holocene
556 environmental variability: the inner N. Iceland shelf (Hunafloi). *Quaternary
557 Science Reviews* 22: 175-193.
- 558 Bâcle JE, Carmack C, Ingram RG (2002) Water column structure and
559 circulation in the North Water during spring transition: April-July 1998. *Deep
560 Sea Research* 49: 4907-4925.
- 561 Bennike O (2004) Holocene sea-ice variations in Greenland: onshore evidence.
562 *The Holocene* 14: 607-613
- 563 Berger A, Loutre MF (1991) Insolation values of the climate of the last 10 million
564 years. *Quaternary Science Reviews* 10: 297-318
- 565 Bindschadler RA (1984) Jakobshavns Glacier drainage basin; a balance assessment.
566 *Journal of Geophysical Research. C. Oceans and Atmospheres* 89: 2066-
567 2072.
- 568 Bindschadler R (2006) Hitting the Ice Sheets Where It Hurts. *Science* 311:1720-1721
- 569 Buch E (1981) A Review of the oceanographic conditions in subarea O and 1 in the

570 decade 1970- 79. NAFO Symposium on Environmental conditions in the
571 Northwest Atlantic during 1970-79. NAFO Scientific Council Studies no.5.
572 Buch E, Pedersen SA, Ribergaard MH (2004) Ecosystem Variability in West
573 Greenland Waters. *Journal of Northw. Atl. Fish. Sci.*34: 13-28.
574 Briner JP, Stewart HAM, Young NE, Philipps W, Losee S (2010) Using proglacial-
575 threshold lakes to constrain fluctuations of the Jakobshavn Isbræ ice margin,
576 western Greenland, during the Holocene. *Quaternary Science Reviews* 29:
577 3861-3874.
578 Caralp MH (1989) Abundance of *Bulimina exilis* and *Melonis barleeaanum*:
579 Relationship to the quality of marine organic matter. *Geo-Marine Letters* 9:37-
580 43.
581 Dahl-Jensen D, Mosegaard K, Gundestrup N, Clow GD, Johnsen SJ, Hansen AW,
582 Balling N (1998) Past temperatures directly from the Greenland Ice Sheet.
583 *Science* 282: 268-271.
584 Duplessy JC, Invanova EV, Murdmaa IO, Paterne M, Labyrie L (2001) Holocene
585 palaeoceanography of the northern Barents Sea and variations of the
586 northward heat transport by the Atlantic Ocean. *Boreas* 30: 2-16.
587 Eiríksson J, Larsen G, Knudsen KL, Hafliðason H, Heinemeier J, Simonarson LA
588 (2004) Marine reservoir age variability and water mass distribution in the
589 Iceland Sea. *Quaternary Science Reviews* 23: 2247-2268.
590 Fredskild B (2000) The Holocene vegetational changes on Qeqertarsuatsiaq, a west
591 Greenland island. *Geografisk Tidsskrift* 100: 7-14.
592 Funder S, Weidick A (1991) Holocene boreal molluscs in Greenland –
593 palaeoceanographic implications. *Palaeogeography, Palaeoclimatology,*
594 *Palaeoecology* 85: 123-35.
595 Funder S, Kjeldsen KK, Kjær, KH, Ó Cofaigh C (2011) The Greenland Ice Sheet

596 During the Past 300,000 Years: A Review. In J. Ehlers, Gibbard PL and
597 Hughes PD, editors: *Developments in Quaternary Science* 15, Amsterdam,
598 The Netherlands; 699-713.

599 Hald M, Steinsund PI (1996) Benthic foraminifera and carbonate dissolution
600 in surface sediments of the Barents- and Kara Seas. *Berichte zur*
601 *Polarforschung* 21: 996.

602 Hald M, Korsun S (1997) Distribution of modern benthic foraminifera from
603 fjords of Svalbard, European Arctic. *Journal of Foraminiferal Research* 27:
604 101-122.

605 Hall IG, Bianchi G, Evans JR (2004) Centennial to millennial scale Holocene climate-
606 deep water linkages in the North Atlantic. *Quaternary Science Reviews* 23,
607 1529-1536.

608 Hansen BW, Nielsen TG, Levinsen H (1999) Plankton community structure and
609 carbon cycling on the western coast of Greenland during the stratified summer
610 situation. III. Mesozooplankton. *Aquatic Microbial Ecology* 16: 233-249.

611 Harff J, Dietrich R, Endler R, Hentzsch B, Jensen J B, Kuijpers A, Krauss N, Leipe T,
612 Lloyd JM, Mikkelsen N, Moros M, Perner K, Richter A, Risgaard-Petersen N,
613 Rysgaard S, Richter T, Sandgren P, Sheshenko V, Snowball I, Waniek J,
614 Weinrebe W, Witkowski A (2007) Deglaciation history, coastal development,
615 and environmental change during the Holocene in western Greenland. *Cruise*
616 *report R/V Maria S. Merian, cruise MSM 05/03.*

617 Heegaard E, Birks HJB, Telford JT (2005) Relationships between calibrated ages
618 and depth in stratigraphical sequences: an estimation procedure by mixed
619 effect regression. *The Holocene* 15: 612-618.

620 Hillaire-Marcel C, de Vernal A, Bilodeau G, Weaver A (2001) Absence of

621 Deepwater formation in the Labrador Sea during the last interglacial period.
622 *Nature* 410: 1073-1077.

623 Hogan K, Dix J, Lloyd J, Long A, Cotterill C (2011) Near surface stratigraphy of
624 eastern Disko Bugt, West Greenland: implications for glacial marine
625 sedimentation. *Journal of Quaternary Science* 26, 757-766.

626 Holland DM, Thomas RH, De Young B, Ribergaard MH, Lyberth B (2008)
627 Acceleration of Jakobshavn Isbrae triggered by warm subsurface ocean
628 waters. *Nature Geoscience* 1: 659-664.

629 Howat IM, Joughin I, Scambos TA (2007) Rapid changes in ice discharge from
630 Greenland outlet glaciers. *Science* 315: 1559-1561.

631 Howat IM, Joughin I, Fahnestock M, Smith BE, Scambos TA (2008) Synchronous
632 retreat and acceleration of southeast Greenland glaciers 2000-06: ice
633 dynamics and coupling to climate. *Journal of Glaciology* 54: 646-660.

634 Ishman SE, Foley KM (1996) Modern benthic foraminifer distribution in the
635 Amerasian Basin, Arctic Ocean. *Micropaleontology* 42: 206-220.

636 Jakobsson M, Macnab R, Mayer L, Anderson R, Edwards M, Hatzky J, Schenke HW,
637 Johnson P (2008). An improved bathymetric portrayal of the Arctic Ocean:
638 implications for ocean modeling and geological, geophysical and
639 oceanographic analyses. *Geophysical Research Letters* 35, L07602.
640 doi:10.1029/2008GL033520.

641 Jennings AE, Helgadóttir G (1994) Foraminiferal assemblages from the fjords and
642 shelf of eastern Greenland. *Journal of Foraminiferal Research* 24: 123-44.

643 Jennings AE, Hagen S, Hardardóttir J, Stein R, Ogilvie AEJ, Jonsdóttir I (2001)
644 Oceanographic change and terrestrial human impacts in a post A.D. 1400

645 sediment record from the southwest Iceland shelf. *Climatic Change* 48
646 (Special Issue, The Iceberg in the Mist: Northern Research in Pursuit of ‘A
647 Little Ice Age’, guest editors Ogilvie AE and Jónsson T), 83-100.

648 Jennings AE, Knudsen KL, Hald M, Hansen CV, Andrews JT (2002) A mid-Holocene
649 shift in Arctic sea-ice variability on the East Greenland Shelf. *The Holocene*
650 12: 49-58.

651 Jennings AE, Weiner NJ, Helgadottir G, Andrews JT (2004) Modern foraminiferal
652 faunas of the southwestern to northern Iceland shelf: oceanographic and
653 environmental controls. *Journal of Foraminiferal Research* 34, 180-207.

654 Jennings AE, Andrews J, Wilson L (2011) Holocene environmental evolution of
655 the SE Greenland Shelf North and South of the Denmark Strait: Irminger and
656 East Greenland current interactions. *Quaternary Science Reviews* 30: 980-
657 998.

658 Jennings AE, Perner K, Moros M, Walton M, Andrews JT, Ó Cofaigh C, in prep.
659 Holocene paleoenvironments and deglaciation history of SW Disko Bugt based
660 on multi proxy analyses. *In preparation for Journal of Quaternary Science*.

661 Jiang H, Seidenkrantz MS, Knudsen KL, Eiríksson J (2002) Late-Holocene summer
662 sea surface temperatures based on a diatom record from the north Icelandic
663 shelf. *The Holocene* 12: 137-147.

664 Joughin I, Abdalati W, Fahnestock M (2004) Large fluctuations in speed on
665 Greenland’s Jakobshavn Isbræ glacier. *Nature* 432: 608-610.

666 Joughin I, Das SB, King MA, Smith BE, Howat IM, Moon T (2008) Seasonal
667 speed up along the western flank of the Greenland Ice Sheet. *Science* 320:
668 781–783.

669 Kaplan MR, Wolfe AP, Miller GH (2002) Holocene environmental variability in

670 southern Greenland inferred from lake sediments. *Quaternary Research* 58:
671 149-159.

672 Kaplan MR, Wolfe AP (2006) Spatial and temporal variability of Holocene
673 temperature trends in the North Atlantic sector. *Quaternary Research* 65: 223-
674 231.

675 Kaufman DS, Ager TA, Anderson NJ, Anderson PM, Andrews JT, Bartlein PJ,
676 Brubaker LB, Coats LL, Cwynar LC, Duvall ML, Dyke AS, Edwards ME, Eisner
677 WR, Gajewski K, Geirsdóttir A, Hu FS, Jennings AE, Kaplan MR, Kerwin MW,
678 Lozhkin AV, MacDonald GM, Miller GH, Mock CJ, Oswald WW, Otto-Bliesner
679 BL, Porinchu DF, Rühland K, Smol JP, Steig EJ, Wolfe BB (2004) Holocene
680 thermal maximum in the western Arctic (0–180°W). *Quaternary Science*
681 *Reviews* 23: 529-560.

682 Kaufman DS, Schneider DP, McKay NP, Ammann CA, Bradley RS, Briffa KR, Miller
683 GH, Otto-Bliesner BL, Overpeck JT, Vinther BM, Arctic Lakes 2k Project
684 Members (2009) Recent warming reverses long-term Arctic cooling. *Science*
685 325: 1236-1239.

686 Knudsen KL, Seidenkrantz MS (1994) *Stainforthia feylingi* new species
687 from arctic to subarctic environments, previously recorded as *Stainforthia*
688 *schreibersiana* (Czjzek). *Cushman Foundation for Foraminiferal Research*
689 *Special Publication* 32: 5-13.

690 Knudsen KL, Stabell B, Seidenkrantz MS, Eiríksson J, Blake Jr W (2008a) Deglacial
691 and Holocene conditions in northernmost Baffin Bay: sediments, foraminifera,
692 diatoms and stable isotopes. *Boreas* 37: 346-376.

693 Knudsen KL, Søndergaard MKB, Eiríksson J, Jiang H (2008b) Holocene thermal

694 maximum off North Iceland: Evidence from benthic and planktonic foraminifera
695 in the 8600-5200 cal year BP time slice. *Marine Micropaleontology* 67: 120-
696 142.

697 Krawczyk D, Witkowski A, Moros M, Lloyd JM, Kuijpers A, Kierzek A (2010) Late-
698 Holocene diatom-inferred reconstruction of temperature variations of the West
699 Greenland Current from Disko Bugt, central West Greenland. *The Holocene*
700 20: 659-666.

701 Kuijpers A, Troelstra SR, Prins MA, Linthout K, Akhmetzhanov A, Bouryak S,
702 Bachmann MF, Lassen S, Rasmussen S, Jensen JB (2003) Late quaternary
703 sedimentary processes and ocean circulation changes at the Southeast
704 Greenland margin. *Marine Geology* 195: 109-129.

705 Lassen SJ, Kuijpers A, Kunzendorf H, Hoffman-Wieck G, Mikkelsen N, Konradi P
706 (2004) Late-Holocene Atlantic bottom water variability in Igaliku Fjord, South
707 Greenland, reconstructed from foraminifera faunas. *The Holocene* 14: 165-
708 171.

709 Levinsen H, Turner JT, Nielsen TG, Hansen BW (2000) On the trophic coupling
710 between protists and copepods in arctic marine ecosystems. *Marine Ecology*
711 *Progress Series* 204:65-77.

712 Lloyd JM, Park LA, Kuijpers A, Moros M (2005) Early Holocene palaeoceanography
713 and deglacial chronology of Disko Bugt, West Greenland. *Quaternary Science*
714 *Reviews* 24: 1741-1755.

715 Lloyd JM (2006) Modern distribution of benthic foraminifera from Disko Bugt, west
716 Greenland. *Journal of Foraminiferal Research* 36: 315-331.

717 Lloyd JM, Kuijpers A, Long A, Moros M, Park LA (2007) Foraminiferal reconstruction
718 of mid- to late-Holocene ocean circulation and climate variability in Disko Bugt,
719 West Greenland. *The Holocene* 17:1079-1091.

720 Lloyd JM, Moros M, Perner K, Telford R, Kuijpers A, Jansen E, McCarthy DJ (2011)
721 A 100 year record of ocean temperature control on the stability of Jakobshavn
722 Isbrae, West Greenland. *Geology* 39: 867-870.

723 Long AJ, Roberts DH (2002) A revised chronology for the 'Fjord Stade' moraine in
724 Disko Bugt, west Greenland. *Journal of Quaternary Science* 17: 561-579.

725 Long AJ, Roberts DH (2003) Late Weichselian deglacial history of Disko Bugt, West
726 Greenland, and the dynamics of the Jakobshavns Isbrae ice stream.
727 *Boreas* 32: 208-226.

728 Moon T, Joughin I (2008) Changes in ice front position on Greenland's outlet glaciers
729 from 1992 to 2007. *Journal of Geophysical Research-Earth Surface* 113
730 F02022, doi: 10.1029/2007JF000927.

731 Moros M, Emeis K, Risebrobakken B, Snowball I, Kuijpers A, McManus J, Jansen E
732 (2004) Sea surface temperatures and ice rafting in the Holocene North
733 Atlantic: climate influences on northern Europe and Greenland. *Quaternary*
734 *Science Reviews* 23: 2113-2126.

735 Moros M, Andrews JT, Eberl DD, Jansen E (2006a) Holocene history of
736 drift ice in the northern North Atlantic: Evidence for different spatial and
737 temporal modes. *Paleoceanography* 21: doi:10.1029/2005PA001214.

738 Moros M, Jensen KG, Kuijpers A (2006b) Mid- to late- Holocene hydrological and
739 climatic variability in Disko Bugt, central West Greenland. *The Holocene* 16:
740 357–367.

741 Moros M, Jansen E, Oppo D, Giraudeau J, Kuijpers A. Reconstruction of the late
742 Holocene changes in the Sub-Arctic Front position at the Reykjanes Ridge,
743 north Atlantic. *The Holocene* (in press).

744 Møller HS, Jensen KG, Kuijpers A, Aagaard-Sorensen S, Seidenkrantz M-S, Prins M,

745 Endler R, Mikkelsen N (2006) Late-Holocene environment and climate
746 changes in Ameralik Fjord, southwest Greenland: evidence from the
747 sedimentary record. *The Holocene* 16: 685-695.

748 Mudie P J, Keen CE, Hardy IA, Vilks G (1984) Multivariate-analysis and
749 quantitative paleoecology of benthic foraminifera in surface and late
750 Quaternary shelf sediments, northern Canada. *Marine Micropaleontology* 8:
751 283-313.

752 Murray JW (1991) *Ecology and palaeoecology of benthic foraminifera*. London:
753 Longman.

754 Oppo DW, McManus JF, Cullen JR (2003) Palaeoceanography: deepwater variability
755 in the Holocene epoch. *Nature* 422: 277-278.

756 Osterman LE, Nelson AR (1989) Latest Quaternary and Holocene paleoceanography
757 of the eastern Baffin Island continental shelf, Canada: benthic foraminiferal
758 evidence. *Canadian Journal of Earth Science* 26: 2236-2248.

759 Perner K, Moros M, Lloyd JM, Kuijpers A, Telford RJ, Harff J (2011) Centennial scale
760 benthic foraminiferal record of late Holocene oceanographic variability in Disko
761 Bugt, West Greenland. *Quaternary Science Reviews* 30: 2815-2826.

762 Polyak L, Solheim A (1994) Late- and postglacial environments in the northern
763 Barents Sea, west of Franz Josef Land. *Polar Research* 13: 197-207.

764 Ren J, Jiang H, Seidenkrantz MS, Kuijpers A (2009) A diatom-based reconstruction
765 of Early Holocene hydrography and climatic change in a southwest Greenland
766 fjord. *Marine Micropaleontology* 70: 166-176.

767 Reimer PJ, Baillie MGL, Bard E, Bayliss A, Beck JW, Blackwell PG, Bronk Ramsey
768 C, Buck CE, Burr GS, Edwards RL, Friedrich M, Grootes PM, Guilderson TP,
769 Hajdas I, Heaton TJ, Hogg AG, Hughen KA, Kaiser KF, Kromer B, McCormac
770 FG, Manning SW, Reimer RW, Richards DA, Southon JR, Talamo S, Turney

771 CSM, van der Plicht J, Weyhenmeyer CE (2009) IntCal09 and Marine09
772 radiocarbon age calibration curves, 0-50,000 years cal BP. *Radiocarbon* 51:
773 1111-1150.

774 Ribeiro S, Moros M, Ellegaard M, Kuijpers A (2012) Climate variability in West
775 Greenland during the past 1500 years: evidence from a high-resolution marine
776 palynological record from Disko Bay. *Boreas* 41: 68-83.

777 Ribergaard MH, Kliem N, Jespersen M (2006) HYCOM for the North Atlantic Ocean
778 with special emphasis on West Greenland Water. *Technical Report 06-0*.
779 www.dmi.dk/dmi/tr06-07

780 Richter TO, Peeters FCJ, van Weering T (2009) Late Holocene (0–2.4 ka BP)
781 surface water temperature and salinity variability, Feni Drift, NE Atlantic
782 Ocean. *Quaternary Science Reviews* 28: 1941–1955.

783 Rignot E, Kanagaratnam P (2006) Changes in the velocity structure of the Greenland
784 Ice Sheet. *Science* 11: 986–990.

785 Rignot E, Koppes M, Velicogna I (2010) Rapid submarine melting of the calving faces
786 of West Greenland glaciers. *Nature Geoscience* 3:187-191.

787 Risebrobakken B, Jansen E, Andersson C, Mjelde E, Hevroy K (2003) A high-
788 resolution study of Holocene paleoclimatic and paleoceanographic changes in
789 the Nordic Seas. *Paleoceanography* 18, 1017-1031.
790 [doi:10.1029/2002PA000764](https://doi.org/10.1029/2002PA000764)

791 Roberts DH, Long AJ (2005) Streamlined bedrock terrain and fast ice flow,
792 Jakobshavns Isbrae, West Greenland: implications for ice stream and ice
793 sheet dynamics. *Boreas* 34: 25-42.

794 Rytter F, Knudsen KL, Seidenkrantz MS, Eiríksson J (2002) Modern distribution of
795 benthic foraminifera on the North Icelandic shelf and slope. *Journal of*
796 *Foraminiferal Research* 32: 217-244.

797 Seidenkrantz MS, Aagaard-Sørensen S, Sulsbrück S, Kuijpers A, Jansen KG,
798 Kunzendorf H (2007) Hydrography and climate of the last 4400 years in a SW
799 Greenland fjord – implications for Labrador Sea palaeoceanography. *The*
800 *Holocene* 17: 387-401.

801 Seidenkrantz MS, Roncaglia L, Fischel A, Heilmann-Clausen C, Kuijpers A, Moros
802 M (2008) Variable North Atlantic seesaw patterns documented by a late
803 Holocene marine record from Disko Bugt, West Greenland. *Marine*
804 *Micropaleontology* 68: 66-83.

805 Sejrup HP, Birks HJB, Klitgaard-Kristensen D, Madsen H (2004) Benthonic
806 foraminiferal distributions and quantitative transfer functions for the northwest
807 European continental margin. *Marine Micropaleontology* 53: 197-226.

808 Sha L, Jiang H, Knudsen KL (2011) Diatom evidence of climatic change in
809 Holsteinsborg Dyb, west of Greenland, during the last 1200 years. *The*
810 *Holocene* 22: 347-358.

811 Steinsund PI, Polyak LV, Hald M, Mikhailov V, Korsun S (1994) Distribution of
812 calcareous benthic foraminifera in recent sediments of the Barents and Kara
813 Sea. In Steinsund PI, Benthic foraminifera in surface sediments of the Barents
814 and Kara Seas: modern and late Quaternary application. Ph.D. thesis,
815 Department of Geology, Institute of Biology and Geology, Univeristy of
816 Tromsø.

817 Straneo F, Hamilton GS, Sutherland DA, Staerns LA, Davidson F, Hammill MO,
818 Stenson GB, Rosing-Asvid A (2010). Rapid circulation of warm subtropical
819 waters in a major glacial fjord in East Greenland. *Nature Geoscience* 3: 182–
820 186.

821 Stuiver M, Reimer PJ (1993) CALIB Radiocarbon calibration program. *Radiocarbon*
822 35: 215-230.

- 823 Tang CCL, Ross CK, Yao T, Petrie B., De Tracey BM, Dunlap E (2004) The
824 circulation, water mass and sea-ice of Baffin Bay. *Progress in Oceanography*
825 63: 183-228.
- 826 Thomas RH (2004) Force-perturbation analysis of recent thinning and acceleration of
827 Jakobshavn Isbræ, Greenland. *Journal of Glaciology* 50: 57-66.
- 828 Vilks G (1980) Postglacial basin sedimentation on the Labrador Shelf. *Geological*
829 *Society of Canada*; 1-28.
- 830 Vilks G (1981) Late glacial–postglacial foraminiferal boundary in sediments of eastern
831 Canada, Denmark and Norway. *Geoscience Canadian* 8: 48-56.
- 832 Vilks G, Deonarine B (1988) Labrador shelf benthic foraminifera and stable oxygen
833 isotopes of *Cibicides lobatulus* related to the Labrador Current. *Canadian*
834 *Journal of Earth Science* 25: 1240-1255.
- 835 Vinther BL, Buchardt SL, Clausen HB, Dahl-Jensen D, Johnsen S J, Fisher DA,
836 Koerner RM, Raynaud D, Lipenkov V, Andersen KK, Blunier T, Rasmussen
837 SO, Steffensen JP, Svensson AM (2009) Holocene thinning of the Greenland
838 ice sheet. *Nature* 461: 385-388.
- 839 Weidick A, Oerter H, Reeh N, Thomsen HH, Thorning L (1990) The recession of the
840 Inland Ice margin during the Holocene climatic optimum in the Jakobshavn
841 Isfjord area of West Greenland. *Palaeogeography, Palaeoclimatology,*
842 *Palaeoecology* 82, 389–399.
- 843 Weidick A, Bennike O (2007) Quaternary glaciations history and glaciology of
844 Jakobshavn Isbræ and the Disko Bugt region, West Greenland: a review.
845 *Geological Survey of Denmark and Greenland Bulletin* 14: 78pp.
- 846 Williamson MA, Keen CE, Mudie PJ (1984) Foraminiferal distribution on the
847 continental margin off Nova Scotia. *Marine Micropaleontology* 9: 219–239.
- 848 Wollenburg J, Knies J, Machensen A (2004) High-resolution palaeoproductivity

849 fluctuations during the last 24 kyr indicated by benthic foraminifera in the
850 marginal Arctic Ocean: 246. *Palaeogeography, Palaeoclimatology,*
851 *Palaeoecology* 204: 209-238.

852 Young NE, Briner, JP, Stewart HAM, Axford Y, Csatho B, Rood DH, Rinkel RC
853 (2011) Response of Jakobshavn Isbræ, Greenland, to Holocene climate
854 change. *Geology* 39: 131-134.

855 Zarudzki EFK (1980) Interpretation of shallow seismic profiles over the continental
856 shelf in West Greenland between latitudes 64° and 69° 30' N. *Geological*
857 *Survey of Greenland Report* 100: 58-61.

858 Zwally HJ, Abdalati W, Herring T, Larson K, Saba J, Steffen K (2002) Surface melt-
859 induced acceleration of Greenland ice-sheet flow. *Science* 297: 218–222.

860 Zweng MM, Münchow A (2006) Warming and freshening of Baffin Bay, 1916-2003.
861 *Journal of Geophysical Research* 111: C07016, doi:10.1029/2005JC003093.
862

863 **Figure captions**

864 **Figure 1:** Schematic bathymetric map of Disko Bugt, adapted from Jakobsson et al.
865 (2008), showing the location of core 343300 (red dot) and 343310 (black star) in
866 south-western Egedesminde Dyb and present day oceanographic setting of the study
867 area. The insert shows schematically the oceanographic setting around Greenland.
868 Abbreviations are as follow: EGC - East Greenland Current; IC – Irminger Current;
869 WGC – West Greenland Current; LC – Labrador Current.

870 **Figure 2: Lithological characterization and age-depth model of gravity core**
871 **343300.** Sediments deposited in the >200 µm fraction (%), number of counted ice-
872 rafted detritus (IRD) >2 mm, the 63-200 µm fraction (%), total organic carbon content
873 (TOC %) and depths of the AMS radiocarbon dates are presented. The age-depth
874 model of the gravity core 343300 is based on linear interpolation between the
875 respective radiocarbon dates. AMS ¹⁴C dates are calibrated with the Marine09
876 (Reimer et al., 2009) calibration curve using Calib602 (Stuiver and Reimer, 1993).
877 For AMS ¹⁴C dates, see Table 1.

878 **Figure 3: Total foraminiferal assemblage (calcareous and agglutinated) from**
879 **site 343310 versus age.** Foraminiferal frequencies are expressed as a percentage
880 of the total specimens counted. Only species with abundance greater than 10% are
881 included. Additionally, the total number of benthic foraminifera counted, number of
882 benthic foraminifera counted per ml wet sediment, the ratio of calcareous vs.
883 agglutinated specimens, number of test linings and grouping of AtIW (red color) and
884 AW (blue color) indicator species, are presented. The light blue (AW) and light red
885 (Atlw) colored plots show the foraminiferal concentration (no. of specimens per ml
886 wet sediment) of the respective groups. Additionally, we present the Shannon-
887 Wiener-Index (S(H)) calculated for the total benthic foraminiferal assemblage.

888 **Figure 4: Agglutinated foraminiferal assemblage from site 343300 versus age.**
889 Foraminiferal frequencies are expressed as a percentage of total agglutinated
890 specimens counted. Only species with abundance greater than 2% are included. Red
891 (blue) colored species are included in the AtlW (AW) group. In addition, the Shannon-
892 Wiener-Index (S(H)) was calculated based on the agglutinated fauna.

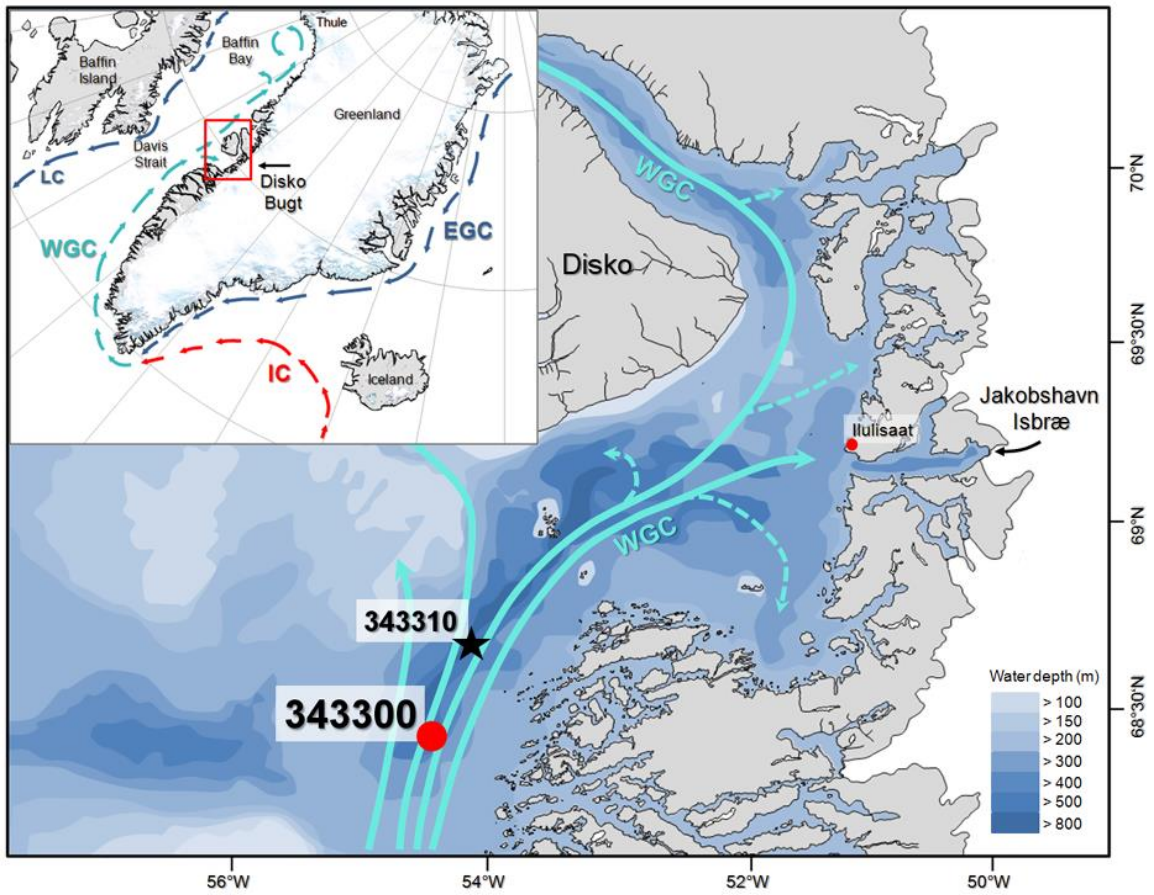
893 **Figure 5: Calcareous foraminiferal assemblage of site 343300.** Foraminiferal
894 frequencies are expressed as a percentage of total calcareous specimens counted.
895 Only species with abundance greater than 2% are included. Red (blue) colored
896 species are included in the AtlW (AW) group. In addition, the Shannon-Wiener-Index
897 (S(H)) was calculated based on the calcareous fauna.

898 **Figure 6: Summary of results compared with other regional data sets.** a) TOC
899 (%) content (343300); b) AMS¹⁴C dates against depth (cm, 343300); c) Sand content
900 (% fraction >63-200 µm; 343300); d) number of calcareous Atlantic water specimens
901 (AtlWcalc) per ml wet sediment, red line displays data from site 343300 and light red
902 line data from nearby site 343310; e) Biogenic carbon (%) content of sediments from
903 site MD99-2322, Denmark Strait (Jennings et al., 2011); f) number of agglutinated
904 Arctic water species (AWagg) per ml wet sediment, blue line displays data from site
905 343300 and light blue line data from nearby site 343310; g) Drift ice proxy data
906 (Quartz%) from core site MD99-2269, NW Iceland (Moros et al., 2006a). Known
907 historical climatic events such as the Roman Warm Period (RWP), the Medieval
908 Climate Anomaly (MCA) and the Little Ice Age (LIA) are marked. The black arrows
909 indicate the position of the two turbidites found in the sediments based on X-ray-
910 radiographs (A. Jennings, unpublished data).

911

912

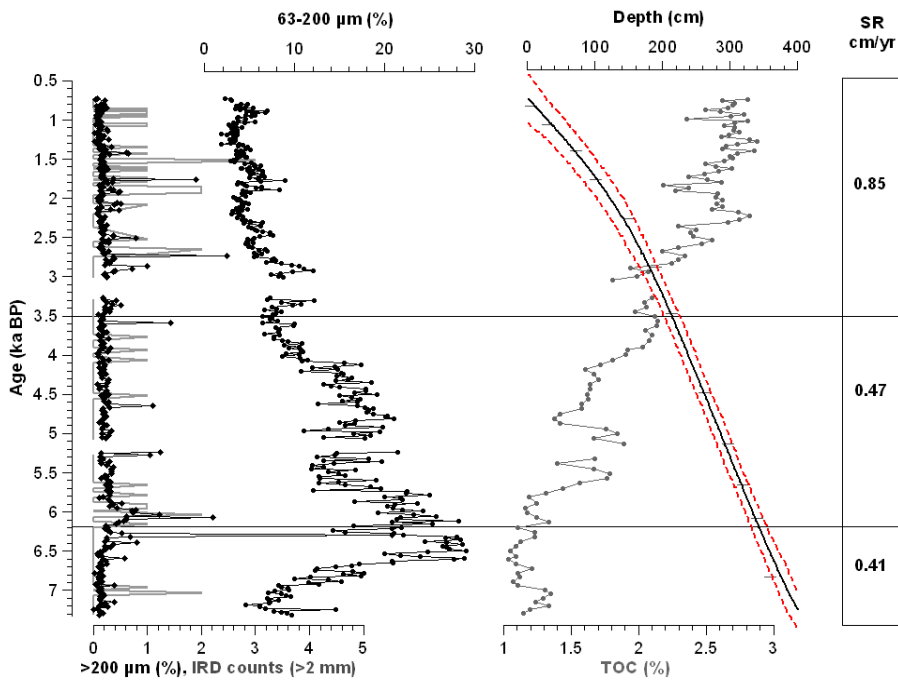
913 Figure 1



914

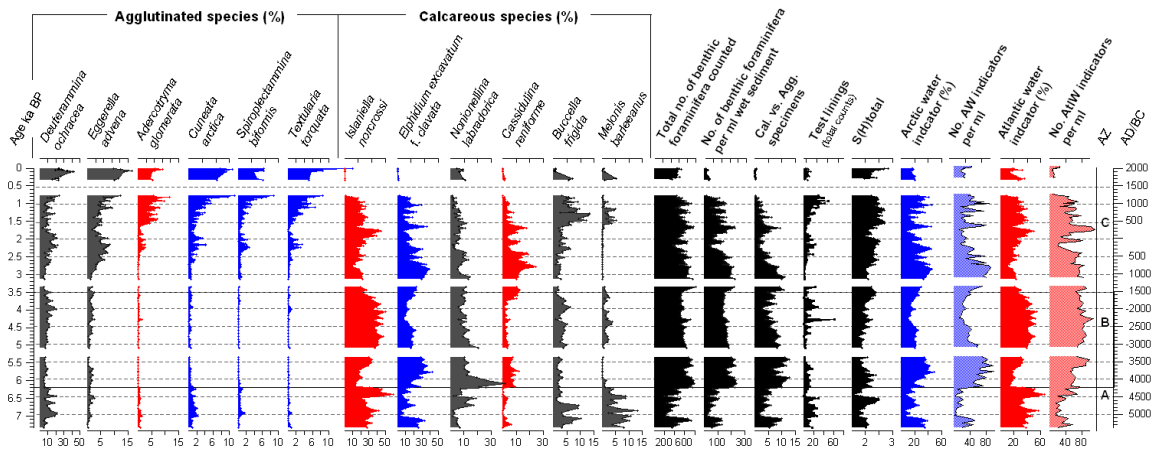
915

916 Figure 2



917

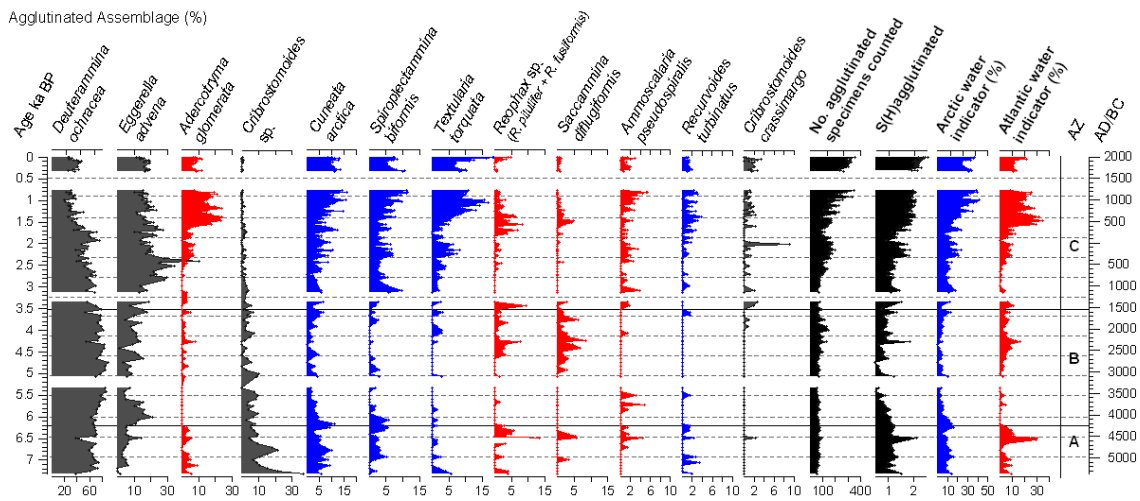
918 Figure 3



919

920

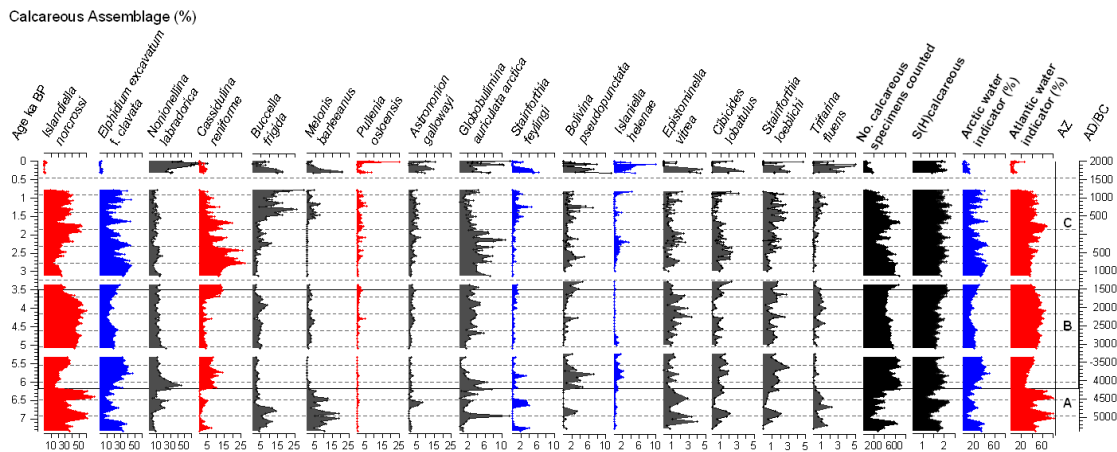
921 Figure 4



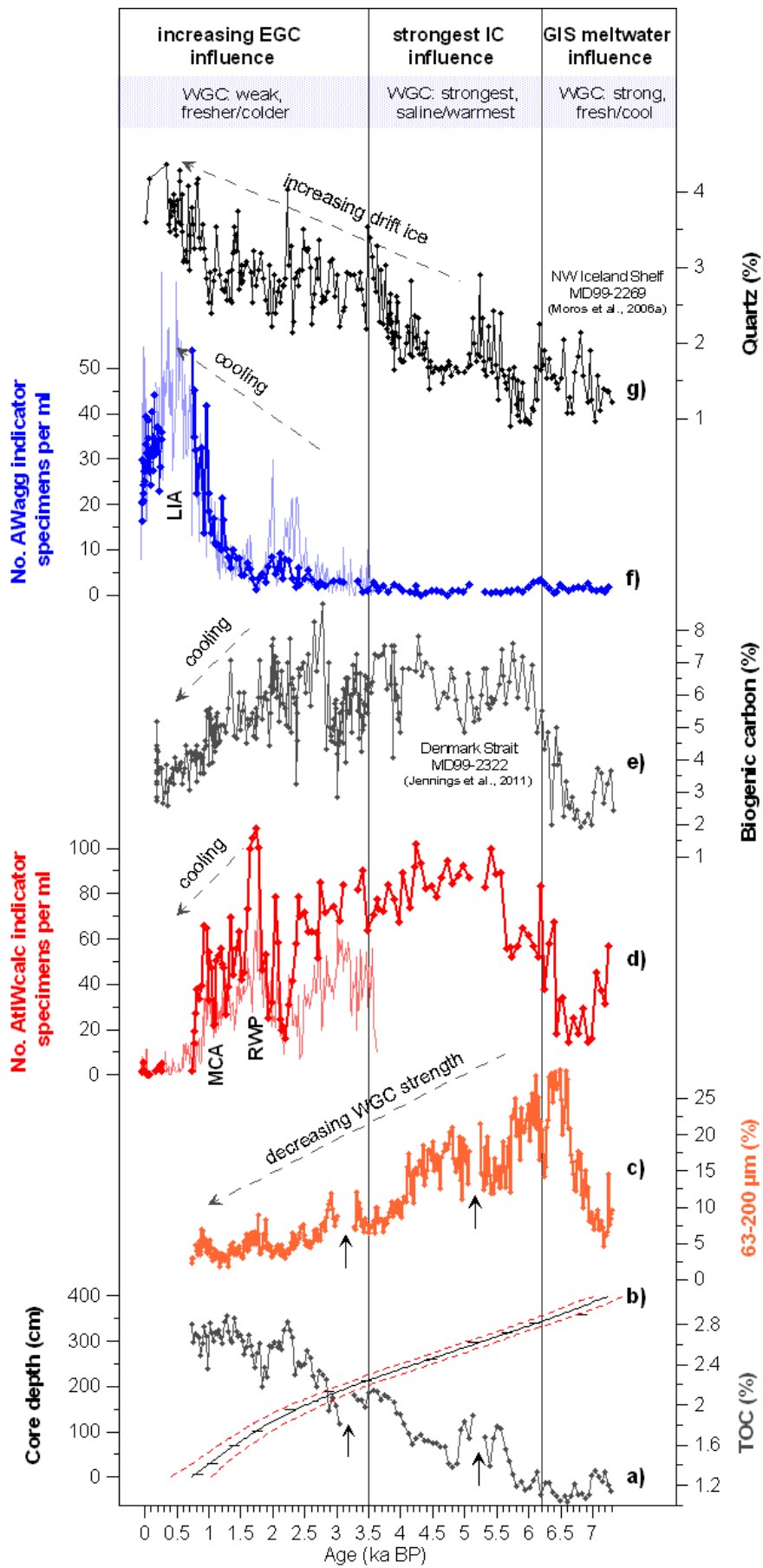
922

923

924 Figure 5



925



928 Table 1 Radiocarbon dates for gravity core 343300. Uncertainties include 68% of the
 929 probability distribution.

Depth (cm)	Lab. Code	Material	Mass mgC	¹⁴ C date years BP	Calibrated yrs BP 1950 ΔR 140±35	Years (AD/BC)
------------	-----------	----------	----------	-------------------------------	-------------------------------------	---------------

MUC 343300-2
(Lloyd et al., 2011)

26.5	Poz-35009	Mix benthic foraminifera	NA	700±30	140-260	AD 1810-1690
------	-----------	--------------------------	----	--------	---------	--------------

GC 343300-3

5.5	Poz-39052	Mix benthic foraminifera	NA	1415±35	767-885	AD 1183-1065
30	Poz-39051	Mix benthic foraminifera	NA	1645±30	990-1117	AD 960-833
71	Poz-33489	Mix benthic foraminifera	NA	1990±50	1324-1466	AD 626-484
100.5	Poz-39047	Mix benthic foraminifera	NA	2305±30	1697-1817	AD 253-133
149.5	Poz-39048	Mix benthic foraminifera	NA	2750±60	2167-2353	217-403 BC
169.5	Poz-43445	Mix benthic foraminifera	NA	3005±35	2561-2713	611-763 BC
190	AA-81304	paired <i>Yoldia limatula</i>	NA	3248±44	2800-2953	850-1003 BC
213.5	Poz-30985	<i>G.auriculata arctica</i> & <i>N. labradorica</i>	NA	3715±35	3401-3532	1451-1582 BC
219.5	Poz-43446	Mix benthic foraminifera	NA	3820±50	3507-3532	1451-1582 BC
239.5	Poz-43447	Mix benthic foraminifera	NA	4110±50	3885-4060	1935-2110 BC
261.5	Poz-33456	<i>G.auriculata arctica</i> & <i>N. labradorica</i>	NA	4490±40	4410-4555	2460-2605 BC
297.5	Poz-33457	<i>N. labradorica</i>	NA	4970±40	5041-5226	3091-3276 BC
319.5	Poz-39053	Mix benthic foraminifera	NA	5440±40	5594-5708	3644-3758 BC
340	AA-81307	<i>G.auriculata arctica</i> & <i>N. labradorica</i>	NA	5822±57	6000-6171	4050-4221 BC
359	Poz-39054	Mix benthic foraminifera	NA	6500±50	6746-6905	4796-4955 BC
399.5	Poz-39055	Mix benthic foraminifera	NA	7390±50	7649-7782	5699-5832 BC

930

931

932

933

934

935

936

937

938

939

940 Table 2 Benthic foraminifera included in the chilled Atlantic water species (AtIW) and
 941 Arctic water species (AW)

Atlantic Water Species (AtIW)	References
Agglutinated	
<i>Adercotryma glomerata</i>	Vilks, 1980; Jennings and Helgadóttir, 1994; Hald and Korsun, 1997; Lloyd, 2006
<i>Ammoscalaria pseudospiralis</i>	Vilks and Deonarine, 1988
<i>Reophax fusiformis</i>	Vilks, 1980; Jennings and Helgadóttir, 1994; Hald and Korsun, 1997
<i>Reophax pilulifer</i>	Vilks, 1980; Jennings and Helgadóttir, 1994; Hald and Korsun, 1997
<i>Saccammina difflugiformis</i>	Vilks, 1980; Scott and Vilks, 1991; Jennings and Helgadóttir, 1994; Hald and Korsun, 1997
Calcareous	
<i>Cassidulina reniforme</i>	Hald and Steinsund, 1996; Guilbault et al., 1997
<i>Pullenia osloensis</i>	Wollenburg et al., 2004
<i>Islandiella norcrossi</i>	Vilks, 1980; Mudie et al., 1984; Hald and Korsun, 1997; Duplessy et al., 2001; Lloyd, 2006
Arctic Water species (AW)	
Agglutinated	
<i>Cuneata arctica</i>	Madsen and Knudsen, 1994, Jennings et al., 2001; Lloyd, 2006
<i>Spiroplectammina biformis</i>	Schafer and Cole, 1986; Jennings and Helgadóttir, 1994; Madsen and Knudsen, 1994; Korsun and Hald, 2000
<i>Textularia torquata</i>	Ishman and Foley, 1996
Calcareous	
<i>Elphidium excavatum</i> f. <i>clavata</i>	Hald and Korsun, 1997; Osterman and Nelson, 1989; Vilks et al., 1989
<i>Islandiella helenae</i>	Korsun and Polyak, 1989; Steinsund et al., 1994
<i>Stainforthia feylingi</i>	Knudsen and Seidenkrantz, 1994

942

943

944

945

946

947

948

949

950

951

952

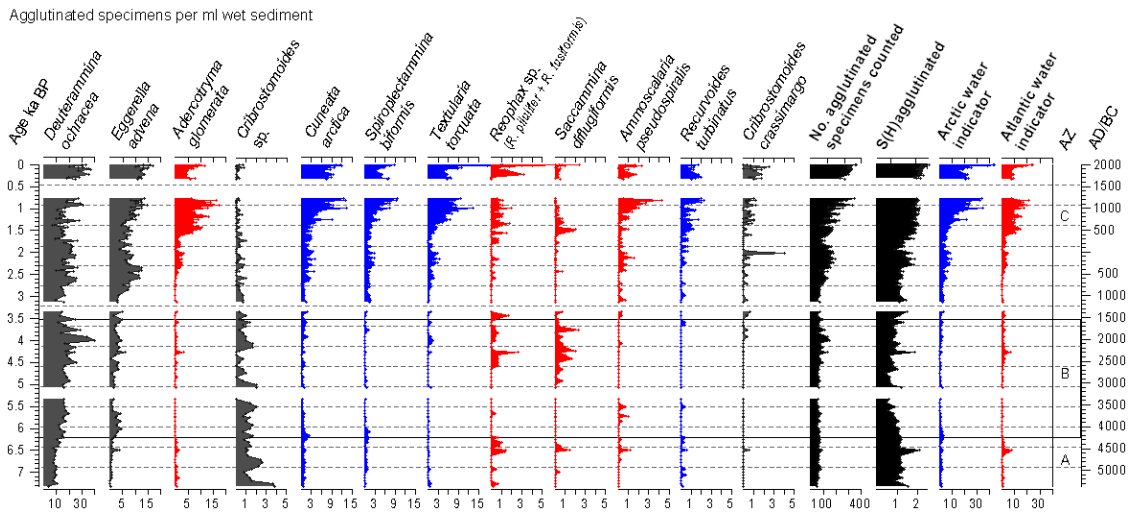
953 **Supplementary figure captions**

954 Figure S1: Agglutinated foraminiferal assemblage from site 343300 versus age.

955 Foraminiferal frequencies are expressed as total number of agglutinated specimens
 956 counted per ml wet sediment. Blue (red) colored species are included in the AW
 957 (AtlW) group.

958 Figure S2: Calcareous foraminiferal assemblage of site 343300. Foraminiferal
 959 frequencies are expressed as total number of calcareous specimens counted per ml
 960 wet sediment. Blue (red) colored species are included in the AW (AtlW) group.

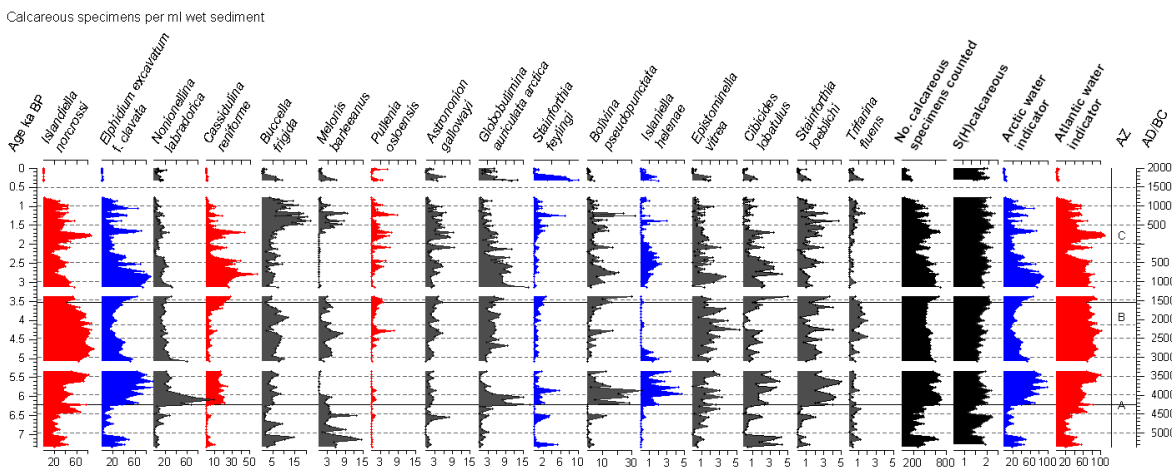
961 **Figure S1**



962

963

964 **Figure S2**



965

